Journal of
Materials Chemistry C

Accepted Manuscript

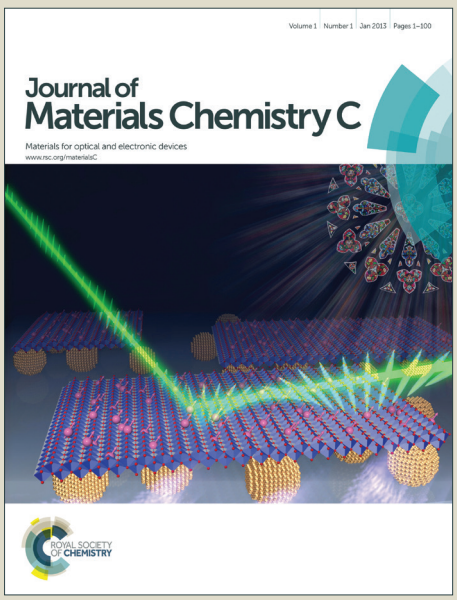




ROYAL SOCIETY OF CHEMISTRY

www.rsc.org/materialsC

Journal Materials Chemistry C

PAPER

# Thermoreversible luminescents ionogels with white light emission: An experimental and theoretical approach

Received 00th January 20xx,
Accepted 00th January 20xx

DOI: 10.1039/x0xx00000x

www.rsc.org/

Talita Jordanna de Souza Ramos,[a] Rodrigo da Silva Viana,[a] Leonardo Schaidhauer,[b] Tania Cassol,[c] Severino Alves Junior[a]

We report here the development of transparent and luminescent ionogels that consist of complexes formed by ionic liquid and lanthanide salts (europium, terbium, or gadolinium). To obtained these soft materials, we use a methodology that involves a room temperature reaction lasting a few minutes and no solvent, stirring or heating. The ionogels exhibit intense emission lines upon UV light irradiation, and were characterized by luminescence spectroscopy made at different temperatures, FTIR, NMR, and Thermogravimetric Analysis. We performed a theoretical study on the luminescent properties of ionogels comparing experimental and theoretical results. The model Sparkle/RM1 was applied to forecast the system geometry and the INDO/S-CIS model was used to calculate the energies of excited states. The intensity parameters were predicted based on the Judd-Ofelt theory and the theoretical model based on 4f-4f transitions was applied in the calculation of transfer fees and energy retrotransference, radioactive and nonradiative decay rates, at last a quantum efficiency. The materials obtained have excellent photophysical properties (lifetime high, narrow line width and high degree of color purity) which makes them extremely valuable for various optical applications.

## 1. Introduction

Consisting of organic salts, the ionic liquids (ILs) have low melting point (below 100°C or even at room temperature). The most common ILs feature an organic cation and an inorganic anion[1]. Initially used as solvents, the ILs won a significant space in several fields over 101 years of existence[2]. The unusual properties attributed to ionic liquids are interesting for synthesis of new inorganic systems[3]. They exhibit features like low viscosity and a high-temperature stability[1],[2]. A wide variety of ILs can be attributed to adequate selection of the anion/cation combination allow to tune the properties of ionic liquids such as polarity, viscosity, among others[4]. Furthermore, many ionic liquids are colorless and transparent through almost the whole visible and near-infrared spectral regions. This fact added with their excellent chemical stability, makes them very useful as optical solvents[5]. Ionic liquids are often considered only solvents but currently, exhibit sophisticated applications in designer Metal Organic Frameworks[6], to raise efficiency of solar cells[7]. One of the most recent employments of ILs is in the formation of soft materials which are luminescent systems with technological potentials[5],[8]. Ionogels are gels obtained by ionic liquids[9],[10]. Today, we are finding ionogels in numerous applications[11],[12]. Because of the ionogels electrochemical characteristics as a high-ionic conductivity, cyclability, wide electrochemical window and a non-flammable[4], we still also cite the use of ionogels like electrolyte supercapacitor[13] or lithium battery electrolyte[4]. The fluorescence enhancement of lanthanides justified employment of ionogels as fluorescence imaging probes for biomedical purposes[14], or yet as luminescence solar concentrators (LSCs)[15-16]. Promising results were obtained for LSCs only the small Stokes shift, the intrinsic dye molecules, induces high self-absorption, which is a significant disadvantage[17]. The use of species with large Stokes shifts change optically active centers, decreasing the losses from

[a] BSTR– Laboratory rare earths, Department of Fundamental Chemistry, Federal University of Pernambuco, Recife- PE, Brazil. E-mail: salvesjr@ufpebr; Fax: +55-81-2126-8442
[b] Departament of Chemistry, Federal University of Rio Grande, Rio Grande – PR, Brazil.
[c] Federal Technological University of Paraná, São Francisco Beltrão – PR, Brazil.
† Electronic Supplementary Information (ESI) available: Synthetic scheme for the luminescent gels, NRM, XRD, TGA, FT-IR, luminescence spectra, details of the structure calculated for the Eu-IL and behavior photoluminescent material under heating. See DOI: 10.1039/x0xx00000x

self-absorption observed with the dyes currently used[17] and quantum dots[18]. In this context, the peculiar emission features typical of lanthanide ions, such as photostability, long lifetimes (>$10^{-4}$ s), large Stokes/anti-Stokes shifts (>200 nm), narrow bandwidth emissions (full width at half-maximum ~1 nm) lying from the UV to the near-infrared (NIR) spectral regions, high luminescence quantum yields[19]. These characteristics explain why lanthanide ions are promising components in LSCs. In order to integrate this class of devices, are being used many efforts to develop new compounds with visible light emission, which is mainly white light generators. For example, in the literature is reported the synthesis of a gelatinous compound formed by the combination of lanthanide complexes ions and molecular organic gelators low-mass preparing luminescent materials that can be potentially applicable in optoelectronics[20].

Even with the large number of luminescent compounds available in the literature, until now, ionogels are not reported among the system components with white light emission.

In this work, we explore the synthesis and characterization of luminescent ionogels was obtained at room temperature without using solvent or agitation. These soft materials are based on lanthanide salts and aprotic functional ionic liquid. The photoluminescence of elaborate compounds is discussed in details and is associated with chemical/thermal stability. Furthermore, we present a structural analysis, and a theoretical study of photoluminescence properties of Ln–IL complexes, which was made to obtain information about the energy transfer process from the ionic liquid for $Eu^{3+}$ ions and using the software LUMPAC[21],[22],[23]. The intensity parameters $\Omega_\lambda$ (λ = 2, 4, and 6) were calculated and compared with the experimental ones. In addition, the $R_{02}$ parameters, radiative and non–radiative decay rates, and experimental emission quantum efficiencies also were investigated. Finally, a white light emitting material was obtained by forming a mixed system comprising the $Eu^{3+}$, $Tb^{3+}$ and $Gd^{3+}$ ions and the ionic liquid: 3-methyl-1H-imidazol-3-ium-1-yl-propane-sulfonate.

## 2. Experimental section

### 2.1. Reagents

The 3-methyl-1H-imidazol-3-ium-1-yl-propane-sulfonate and lanthanide salts ($LnX_3.6H_2O$ were Ln = Eu, Tb or Gd, and X = $NO_3^-$ or $Cl^-$) were prepared according to the reported procedures. All chemicals were purchased from commercial sources: 1–methyl imidazolium and 1,3–propanosulfone (Aldrich), ethyl acetate (Vetec), nitric acid/hydrochloric acid (Dinâmica) and lanthanides oxides (Alfa aesar/Aldrich).

### 2.2. Characterization

For a complete characterization of the material we used nuclear magnetic resonance (NMR), infrared spectroscopy (FTIR), and thermogravimetric analysis (TGA). In NMR deuterated dimethylsulfoxide (99%, Aldrich) were used. The spectrometer is VARIAN model Unity Plus 300 and 400 MHz for $^1H$, to $^{13}C$. The chemical shift values are expressed parts per million (ppm) and coupling constants (J) in Hertz (Hz). The multiplicities are abbreviated as follows: singlet (s), doublet (d), triplet (t), and multiplet (m). Analysis of vibrational modes in the FT–IR (4000 $cm^{-1}$ to 500 $cm^{-1}$) were made by Infrared Spectroscopy Fourier transform spectrometer using a PerkinElmer Spectrum 400 FT-IR/FT-NIR spectrometer. TGA data under an $N_2$ atmosphere were obtained with a Shimadzu TGA 50-H thermogravimetric analyzer, up to a temperature of 800 °C, at a heating rate of 5 °C $min^{-1}$. For the luminescence spectra the samples were excited using a 450 W xenon lamp. The emission and excitation spectra were analyzed using a modular spectrofluorometer Horiba-Jobin Yvon Fluorolog-3 with double excitation, fitted with a 1200 groves/mm grating blazed at 330 nm, and a single emission spectrometer (TRIAX 320) fitted with a 1200 groves/mm grating blazed at 500 nm coupled to a R928P Hamamatsu photomultiplier. All emission spectra were corrected for the spectral response of the monochromators and the detector using typical correction spectra provided by the manufacturer. The experiments with temperature variation used a temperature control module, fixed to the horizontal specimen holder coupled to the spectrofluorimeter previously mentioned. It samples were deposited on glass slides 20 mm in diameter, where the compounds could be illuminated with xenon lamp.

For the lifetime experiments is used the same spectroscopic apparatus using this time a 450 W xenon lamp in its pulsed mode. The lifetime of $Eu^{3+}$ was obtained by monitoring the $^5D_0 \rightarrow {}^7F_2$ (612 nm) emissions upon excitations at 395 nm. For the lifetime of $Tb^{3+}$ was obtained by monitoring the $^5D_4 \rightarrow {}^7F_5$ (542 nm) emissions upon excitations at 370 nm.

The emission quantum efficiency (η) was calculated from Equation 1, where $A_{rad}$ is the radiative decay rate, given by the sum of the spontaneous emission coefficients ($A_{J's}$) $A_{rad} = \sum_{J=1}^{4} A_J$. The total radiative decay rate ($A_{total}$) is given by the relation $A_{total} = \tau^{-1}$, where τ is lifetime for the radiative decay associated with the transition $^5D_0 \rightarrow {}^7F_2$. Finally, the non-radiative decay rate ($A_{nrad}$) is given by the difference $A_{nrad} = A_{total} - A_{rad}$[24].

$$\eta = \frac{A_{rad}}{A_{rad} + A_{nrad}} \quad \textbf{(Equation 1)}$$

## 3. Results and discussion

### 3.1. Synthesis and characterization

The first step is a synthesis of IL. In a 50 ml flask equipped with reflux condenser and oil bath was mixed 10 mmol of 1–methyl imidazolium and 10 mmol of 1,3–propanosultone as available in Fig. S.1. The mixture was conditioned under magnetic stirring at 80° C for 24 hours. The solid obtained is washed three times with 20 mL of ethyl acetate (Vetec) to remove any



 

possible remaining starting material. The resulting product yielded 89% in mass. The lanthanide salts were obtained by a well-established procedure in the literature[25]. To obtain the luminescent materials we used two approaches: heating with stirring and gentle methodology. The latter was chosen to develop samples presented in this paper since it takes place at room temperature, lasts only a few minutes and using no solvent. We used the proportion of 1 mmol of $LnX_3.6H_2O$ (where Ln = Eu, Tb or Gd, and X= $NO_3^-$ or $Cl^-$) to 3 mmol of ionic liquid, and within a few minutes the mixture became homogeneous, the measure by which the system absorbs moisture. We obtained transparent and luminescent gels. Eu–IL emits red emissions irradiated by UV-lamp. Alike substitution of $Eu^{3+}$ with $Tb^{3+}$ results in similar gels (Tb–IL) but with bright green emission under UV light. The Gel with emission in the blue region include Gd–IL. These materials (presented in Fig. SI.1) are conditioned in a desiccator under vacuum.

The ionic liquid development consists of imidazolium cation and an organic substituent with an inorganic sulphate terminal to make it more reactive. As reported in literature, sulfonates groups generally show more promise for dynamic materials where structural pliancy is desired[26]. This justifies the choice of ionic liquid structure to elaborate soft materials. To characterize and check the product's purity and complexes formed, we performed the IR and NMR analysis to ionic liquid and luminescent materials. NMR spectra are contained in Fig. S3-7 and infrared spectroscopy (Fig. 1). The resolution of the structure conforms to the expected result previously reported[27],[28] even after obtaining the luminescent materials. FTIR spectrum, shown in Fig. 1, of the IL and luminescent materials, is characterized by the absorption bands around 3090 $cm^{-1}$ and is consistent for deformations C–H bonds in imidazole ring[27]. The stretch in 1460 $cm^{-1}$ for $CH_2$, 1650 $cm^{-1}$ is attributed to C=C and/or C=N[28]. Bands in 1575 $cm^{-1}$ can be attributed to ring stretching of the imidazolium of the IL. We observed the stretching symmetrical 1035 $cm^{-1}$ and 1180/1300 $cm^{-1}$ asymmetric, which can be applied to stretch S=O as noted earlier[10]. The region between 750–1000 $cm^{-1}$ is consistent to S–O stretch. All of these stretches are kept in luminescent materials, and identified as compatible shift to stretching S=O[28]. This suggests the lanthanide coordination with oxygen belonging to sulfone terminal. The little displacement to stretching S=O is explained due to weak coordination with the metal sulfonate group[26]. We still observed broadband at 3500 $cm^{-1}$ which corresponds to O–H water, and indicates an increase in the hydrophilic character of luminescent materials in relation to ionic liquid. The streching identified at approximately 3200 $cm^{-1}$ N–H indicates the intermolecular hydrogen bond in the gel phase, as previously reported[29].

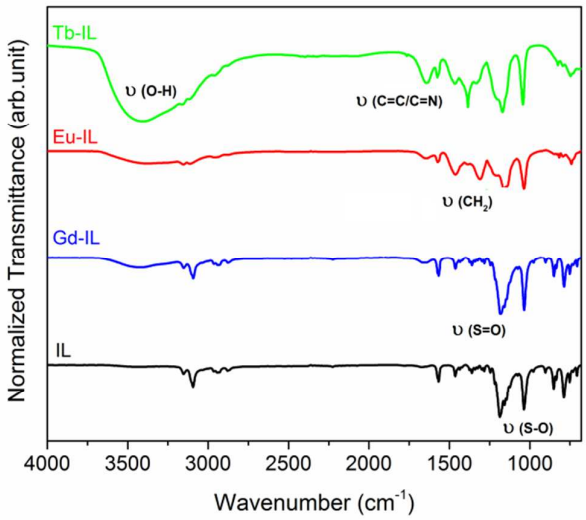


**Fig. 1** Infrared spectrum for IL, Gd–IL, Eu–IL and Tb–IL.

Hydrophilic gels, or xerogels, are quite delicate to analysis because of their ability to absorb moisture from the air, specifically ionic liquids containing the C—N—C—C torsion angle of 100.05° allows the positively charged imidazolium head group and the negatively charged sulfonate group to interact with neighboring zwitterions, forming a C—H···O hydrogen-bonding network[30], this explains the pronounced widening of stretch bands of luminescent materials in infrared spectrum.

### 3.1. Thermal Behavior

Thermalgravimetric analysis is applied to investigate the thermal stability of the luminescent materials, shown in Fig. S8. To IL (black line) we observed the first event a lightweight moisture loss (3%) in approximately 105 °C. The second event shows the degradation for organic structure (80%) until 400 °C. To materials with lanthanides ions (Gd–IL, 7%, Tb–IL, 9%, and Eu–IL, 6%) we see four events. Initially, a moisture loss at 134 °C is most significant for samples with a higher water uptake as shown by broadband at 3500 $cm^{-1}$ in FTIR. The incorporation of lanthanide in IL can improve the thermal stability of the organic compound as observed from the TG curves. For the luminescent material Gd–IL, the event found at 249 °C is associated with degradation to methyl, followed by propane chain (~315 °C). Thermal degradation to imidazole ring was identified at 544 °C and terminal sulfonate at 650°C. For compounds Tb–IL, and Eu–IL, we observed degradation of propane chain and methyl terminal (~272 °C). The thermal decomposition of the imidazolium ring is identified at 600 °C and the sulfonate terminal is degraded at 642 °C. For all luminescent materials the event identifies at 320 °C and indicates the removal of $NO_3^-$, as first observed[31].

### 3.2. Spectroscopic properties

The luminescence of materials ionic liquid (IL) and Gd–IL were investigated from excitation and emission spectra (Fig. 2).

Excitation spectra of IL show the presence of a band centered at 369 nm, which is typically associated with the transition π→π* of the imidazole ring[32], in our case, assigned to IL, the ligand used.

The relaxation of the excited state induces the formation of the band centered at 450 nm in emission spectrum. The luminescence comparison of Gd–IL (with $\lambda_{Ex}$ = 350 nm and $\lambda_{Em}$= 428 nm) in relation to free ligand shows a displacement between the excitation and emission bands to shorter wavelengths, $\Delta\lambda_{Em}$ =19 nm and $\Delta\lambda_{Ex}$ =22 nm. This suggests ligand modification with the coordination compound.

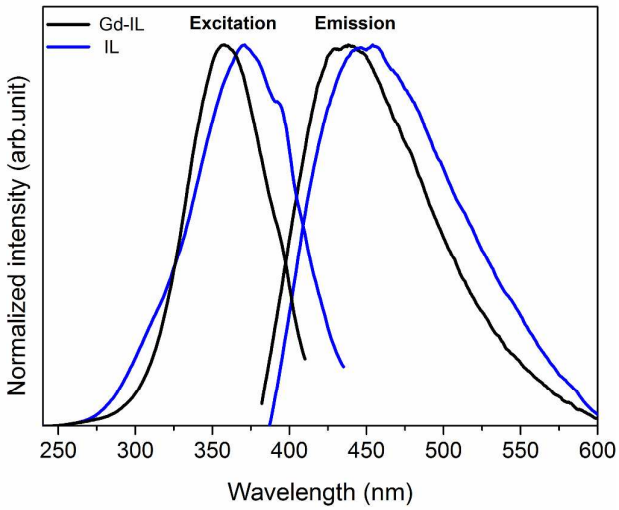


**Fig. 2** Excitation and emission spectra for IL in blue line ($\lambda_{ex}$= 369 nm; $\lambda_{em}$= 450 nm) and Gd–IL in black line ($\lambda_{ex}$= 350 nm; $\lambda_{em}$= 428 nm).

The excitation spectrum of Eu–IL was obtained by monitoring the wavelength of $Eu^{3+}$ ion at 612 nm (black line in Fig. 3). This spectrum shows the lines $^7F_{1,0}\rightarrow{}^5D_{4-0}$, $^5L_6$, $^5G_J$ e $^5H_{3,6}$, typical of intra-4f$^6$ transitions to $Eu^{3+}$ ions situated in the region of 310-547 nm. The emission spectrum of Eu–IL was realized by excitation of $^7F_0\rightarrow{}^5L_6$ transition ($\lambda_{ex}$ = 395 nm), as shown in the red line of Fig. 4. The graphic shows the $^5D_0\rightarrow{}^7F_J$ characteristic transitions (J = 0, 1, 2, 3 e 4) for the trivalent europium. The presence of the $^5D_0\rightarrow{}^7F_0$ transition ($\lambda_{em}$= 578 nm) indicates the absence of inversion in the center of the surrounding environment $Eu^{3+}$ ion. This restricts the symmetry of the metal center for groups similar of these $C_1$, $C_n$, $C_{nv}$, Cs. The spectrum also shows the $^5D_1\rightarrow{}^7F_2$ transition, which suggests non–radiative deactivation processes are not as influential in this system, and may be related to low frequency phonons formed to structural compound[33].

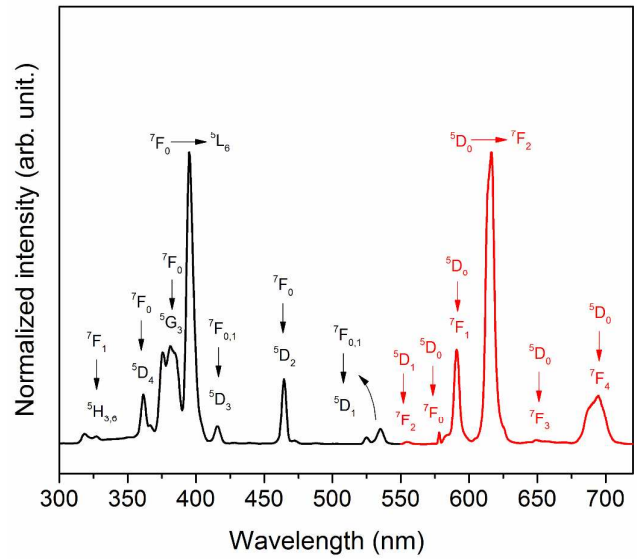


**Fig. 3** Excitation (black line; $\lambda_{em}$ = 616 nm) and emission (red line; $\lambda_{ex}$ = 395 nm) spectra for Eu–IL.

The Eu–IL showed a great chemical stability to present exactly the same spectral emission even one year after the synthesis of the material (Fig. 4).

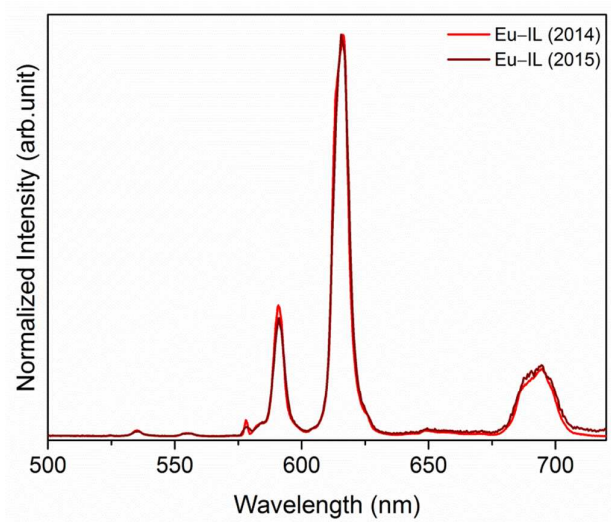


**Fig. 4** Comparision of emission spectrum for Eu-IL (λexc = 395 nm) obtained for over one year after synthesis.

The excitation ($\lambda_{em}$= 542 nm) e emission ($\lambda_{ex}$ = 370 nm) spectrum of Tb–IL were obtained at room temperature and shown in Fig. 5. The excitation spectrum (black line) has lines in the region from 240 nm to 570 nm, which related to the intraconfigurational transitions *f-f* for the $Tb^{3+}$ ion. The emission spectrum (green line in Fig. 4) contains the typical signs of $^5D_4\rightarrow{}^7F_J$ transition (J = 0, 1, 2, 3, 4, 5 e 6), where the transition is more intense and more meaningful for the green emission in the $^5D_4\rightarrow{}^7F_6$.

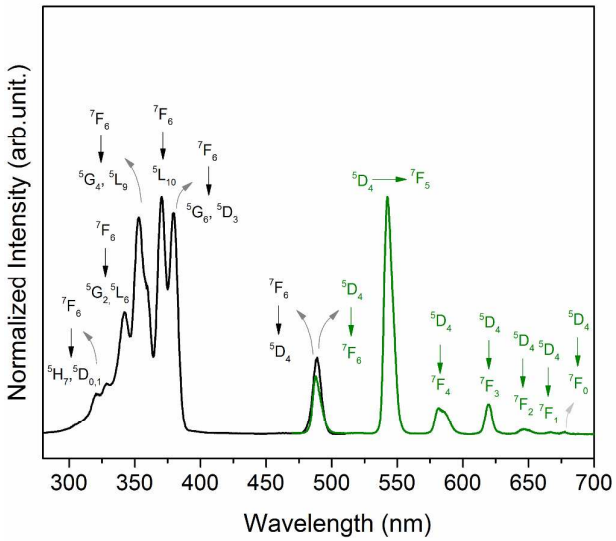


**Fig. 5** Excitation (black line; $\lambda_{em}$ = 542 nm) and emission (green line; $\lambda_{ex}$ = 370 nm) spectra for Tb–IL.

### 3.3. Thermal behavior and reversibility of the materials

The correlation of luminescence effect due to heating of the material can be important in the applications of ionogels. Therefore, the thermal stability of the luminescent materials, up to 250 °C, led to the development of a methodology to study the photophysical properties under temperature variation. The characterization of the photophysical effect under temperature variation for Gd–IL, Eu–IL and Tb–IL was performed by analyzing their emission spectra in the heating range from room temperature to 250°C, at a rate of 1°C/min. In Fig. S12, Gd–IL emission spectra show enlargement while the sample is heated. The spectra show displacement $\Delta\lambda_{em}$ = 17 nm, the initial state to the final state, which must be related to the ligand conformation change in the coordination compound.

The compound Eu–IL does not show changes in the pattern of its excitation spectrum for heating up to 150°C. At temperatures above 150 °C we observed the appearance of a broad band in the region of 300–400 nm (Fig. S13) which relates to the partial degradation of the ligand and the appearance of new intraconfigurational transitions belonging to the species generated. Emission spectra did not show significant changes in their line pattern during heating (Fig. S14), but displayed a slight narrowing of the linewidth related to the removal of moisture from the material. The $^5D_1 \rightarrow {}^7F_2$ transition was also monitored for heating (Fig. S15), where it was observed that maintaining the transition with the temperature rise indicates that the increase of the vibrational frequency in the compound is not sufficient to cause deactivation of this transition.

For the calculation of spectroscopic proprieties of $Eu^{3+}$ we used the Judy–Ofelt parameters[34]-[35]. The experimental values for the ratio of the integrated areas of the transitions $^5D_0 \rightarrow {}^7F_2$ against $^5D_0 \rightarrow {}^7F_1$ ($R_{02/01}$), radiative ($A_{rad}$) and non–radiative ($A_{nrad}$) decay rates and quantum efficiency of emission (η) for compound Eu–IL, depending on the heating temperature, are shown in Table 1.

**Table 1** The experimental values for the ratio of the integrated areas of the transitions $^5D_0 \rightarrow {}^7F_2$ against $^5D_0 \rightarrow {}^7F_1$ ($R_{02/01}$), radiative ($A_{rad}$) and non–radiative ($A_{nrad}$) decay rates and quantum efficiency of emission (η) for compound Eu–IL depend on the heating temperature.

| | $A_{rad}$ ($s^{-1}$) | $A_{nrad}$ ($s^{-1}$) | τ (ms) | η (%) | $R_{02/01}$ |
|---|---|---|---|---|---|
| RT | 355.85 | 3991.98 | 0.233 ± 0.001 | 8.2 | 4.48 |
| 50 °C | 449.65 | 2928.70 | 0.296 ± 0.007 | 13.3 | 5.25 |
| 100 °C | 508.86 | 680.20 | 0.841 ± 0.017 | 42.8 | 5.86 |
| 150 °C | 538.33 | 396.25 | 1.070 ± 0.014 | 57.6 | 6.37 |
| 200 °C | 513.88 | 243.69 | 1.317 ± 0.028 | 67.8 | 6.61 |
| 250 °C | 607.39 | 212.29 | 1.217 ± 0.057 | 74.1 | 7.17 |

The lifetime values for the $^5D_0$ emitting state were determined by the exponential decay curve. The curve showed monoexponential fit for all materials (Fig. S16), indicating the occupation of only one symmetry site for Eu–IL, even after heating, which was expected for a metal complex. The emission quantum efficiency shows a gradual increase in the same step in which Eu–IL is subjected to higher temperatures. This phenomenon is associated with the elimination of water molecules present in the material, due to removal of –OH oscillators that promote energy deactivation of the excited states of $Eu^{3+}$ ion by non–radiative processes. This also can be verified by the significant decrease in non–radiative decay rate ($A_{nrad}$) when heating the material. Moreover, we observed that the chemical environment of $Eu^{3+}$ has symmetry modification, moving toward lower symmetry, as temperatures rise in the compound. This is indicated by increased values of $R_{02/01}$ to Eu–IL on higher temperatures.

The spectroscopic behavior of the Tb–IL compound was also evaluated according to temperature. As occurred in the spectrum of compound Eu–IL, the heating of Tb–IL material does not cause changes in the pattern of excitation spectrum when temperatures are lower than or equal to 150°C, as shown in Fig. S17. However, for higher temperatures we observed the formation of a broad band in the region of 275–400 nm. This affects the transitions arising from the new transitions and correlates with the disposal of the ligand in the material. There are no significant changes in the emission line pattern of the compound Tb–IL (Fig. S18). However there was an increase in the provision of their lifetimes as the heating temperature of the material rose, as viewed in Fig. S20 and Table 2.

The compounds Eu–IL and Tb–IL experience significant reduction of their lifetime at the temperature of 250°C, as well as the emergence of a broad band in their excitation spectra. These are evidences of structural degradation, as indicated in the most significant event in the thermogravimetric analysis (Fig. S8).

**Table 2** Lifetimes of Tb–IL a function of temperature

| Temperature | τ (ms) |
|---|---|
| RT | 0.661 ± 0.017 |
| 50 °C | 0.854 ± 0.007 |
| 100 °C | 0.983 ± 0.008 |
| 150 °C | 1.255 ± 0.007 |
| 200 °C | 1.265 ± 0.015 |
| 250 °C | 0.972 ± 0.019 |

The reversibility of Eu–IL and Tb–IL compounds was evaluated by the heating process at 100°C and subsequent exposure of the material to atmospheric moisture for 24 hours. It is observed that the systems had elevated their lifetimes (τ = 0.84 and 0.98 ms for Eu–IL and Tb–IL respectively) and modification of the profiles of the excitation and emission spectra when subjected to heating. When the gels are exposed to moisture, their lifetimes return to the initial values (τ = 0.23 and 0.66 ms for Eu–IL and Tb–IL respectively) indicating the occurrence of a hydration-dehydration mechanism, activated by the temperature as shown in Fig. S20–S25. This reversibility behavior detected in the photoluminescence favors the use of these compounds as moisture sensors for qualitative measures.

### 3.4. Theoretical approach

The structure of the complex was optimized via Sparkle/RM1 (Fig. 6A). The theoretical structure of the Eu–IL compound presents the metallic center Eu coordinated with nine oxygen atoms, where four bonds are composed of two IL ligands, connected in the form of chelate coordination compound, and five coordination waters (Fig. 6B).

The ligand coordination comes from its sulfone group, as predicted by analysis by FTIR. The sulfur forms a tetrahedral site where one of the oxygen atoms is free and assists the formation of the metal center symmetry. The coordination polyhedron is organized in a distorted symmetry capped square antiprism, which indicates that the arrangement is in point group symmetry close to $C_{4V}$[36]. This symmetry is consistent with the estimate obtained by the emission spectrum of the compound. The distances between the metal center and the oxygen atoms from the coordinated water showed values equal to 2.510, 2.509, 2,508, 2.508 and 2.510Å to Eu1–O61, Eu1–O64, Eu1–O55, Eu1–O58 and Eu1–O52, respectively. All these distances are in agreement with values reported in literature for hydrated complexes of lanthanides[37] (Fig. S26). The metal-ligand distance of O-donors from the ionic liquids have values equal to 2.527, 2.523, 2.520 and 2.520Å to Eu1–O21, Eu1–O22, Eu1–O11 and Eu1–O12 respectively. These values are slightly higher than those found for the oxygen atoms of the coordination water. This can be explained by the reduction of covalent binding character O-Eu and by the high electronegativity of sulfur which increases the ionic character of the bond S-O. However, values for Eu–O are in agreement with the distances identified by the crystallographic information structures with sulfonate/phosphate terminal coordinates with the lanthanide ion[38],[39].

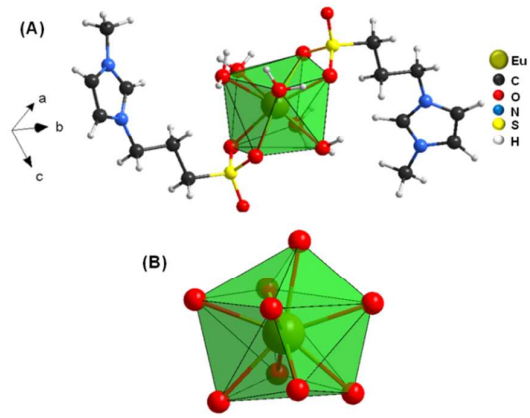


**Fig. 6** Calculated geometry from ground-state using the Sparkle/RM1 model, for the Eu–IL system. In (A) is showed the coordination environment for $Eu^{3+}$ ion and (B) its coordination polyhedron.

Triplet energies are calculated by INDO/S (intermediate neglect of differential overlap/spectroscopic) methodology but hundreds of times faster. Moreover, the semi-empirical results not only reproduce the experimental values but also help explain the values of quantum efficiency observed for these complexes[40]. The other results were calculated using LUMPAC[22].The calculated values of intensity parameters $\Omega_2$, $\Omega_4$, and $\Omega_6$, radiative ($A_{rad}$) and non–radiative ($A_{nrad}$) decay rates and quantum efficiency (η) are exhibited in Table 3 and are in agreement with those obtained experimentally, evidencing the accuracy of the theoretical methodology.

**Table 3** Theoretical and experimental intensity parameters $\Omega_2$, $\Omega_4$, and $\Omega_6$, radiative ($A_{rad}$) and non-radiative ($A_{nrad}$) decay rates and quantum efficiency (η).

| Eu–IL | Intensity parameters ($10^{-20}$ cm$^{-1}$) | | | $A_{rad}$ ($s^{-1}$) | $A_{nrad}$ ($s^{-1}$) | τ (ms) | η (%) |
|---|---|---|---|---|---|---|---|
| | $\Omega_2$ | $\Omega_4$ | $\Omega_6$ | | | | |
| Experimental | 7.13 | 5.67 | - | 355.85 | 3991.98 | 0,23 | 8.18 |
| Sparkle/RM1 | 7.33 | 5,67 | 0.25 | 349.42 | 3952.02 | – | 7.34 |

The intramolecular energy transfer (ET) and back transfer (BT) for Eu–IL were calculated considering that the $Eu^{3+}$ levels arise from the metal ion at an intermediate coupling. The energy of the ligand singlet state must be lower than 38.000 cm$^{-1}$, and the triplet level of the lowest energy must be related to the singlet state previously chosen. The values of energy transfer rates are exhibited in Table 4. This evidence together strengthens the hypothesis that the vibronic coupling of the O–H oscillators from the aqua ligands and the triplet $^5D_{1,0}$ resonance acted as efficient non–radiative channels for $Eu^{3+}$ emission, thus providing a plausible explanation for the short

lifetime and low experimental quantum efficiency. The high values of $A_{nrad}$ are in accordance with this fact.

The difference between experimental and theoretical values may be attributed to the theoretical model that does not consider the role of phonon assistance in the IL→$Eu^{3+}$ energy transfer, as previously reported[21]. Values shown, in Table 4, may distance the experimental values but still show a solid approach when compared to other theoretical approaches described in literature[40],[41],[42]. The theoretical model used provides a sound estimate for the quantum efficiency and facilitates the construction of the power transfer diagram. The theoretical data indicate that the energy transfer occurs from the triplet state of the IL ligand to $^5D_1$ and $^5D_0$ states of $Eu^{3+}$ ion. Furthermore, it is possible to observe that the RL values, i.e., the distance from the donor state (from organic ligand) in relation to the nucleus formed by $Eu^{3+}$ ion, are somewhat higher for the triplet state as determined for the state singlet (Table 3). The triplet state of the complex Eu–IL (18469.80 $cm^{-1}$) was below the $^5D_1$ state (18691.59 $cm^{-1}$), yet the mechanism of energy transfer ($W_{ET1}$) $T_1 \rightarrow {}^5D_1$ is favored. The mechanism of energy back-transfer ($W_{BT1}$) $^5D_1 \rightarrow T_1$ presents the energy transfer rate with an order of magnitude greater than the $W_{ET1}$, which should act in the depopulation of the $^5D_1$ level. On the other hand, the mechanism of energy transfer rate ($W_{ET2}$) $T_1 \rightarrow {}^5D_0$ is favored because of resonance conditions between the states and the exchange mechanism. The $W_{ET2}$ is on the order of $10^6$ $s^{-1}$, which is the same magnitude non–radiative decay rates of $^5D_1 \rightarrow {}^5D_0$ found in coordination compounds[34], which implies the simultaneous occurrence of the two deactivations. In Fig. S27, we present every possible energy transfer mechanism for complex Eu–IL and a diagram of energy levels.

**Table 4** Calculated values of intramolecular energy transfer ($W_{ET}$) and back-transfer ($W_{BT}$) rates optimized by Sparkle/RM1 model.

| Ligand state ($cm^{-1}$) | | 4f state ($cm^{-1}$) | Transfer rate ($s^{-1}$) | Back-transfer rate ($s^{-1}$) |
|---|---|---|---|---|
| Singlet (37135.20) | → | $^5D_4$ (27700.83) | $9.59 \times 10^2$ | $1.19 \times 10^{-21}$ |
| Triplet (18469.8) | → | $^5D_1$ (18691.59) | $1.21 \times 10^9$ | $2.16 \times 10^{10}$ |
| Triplet (18469.8) | → | $^5D_0$ (17301.04) | $2.17 \times 10^9$ | $7.85 \times 10^6$ |

Analysis of the modified local symmetry of $Eu^{3+}$ ion was conducted with Eu–IL compound in a liquid phase and gel form. It is noted that the system adopts the highest symmetry that the $C_{4V}$ when the compound is in liquid phase, as indicated by modification patterns of excitation and emission spectra (Fig. S28-S29) and the integrated area ratios $R_{(02/01)}$(solution) = 0.84 and $R_{(02/01)}$(RT) = 4.48. In increased hydration, the compound promotes the reduction of their lifetime for $\tau$ = 0.13 ms (Fig. S30), which is associated with increased –OH oscillators in the system.

### 3.5. Ionogel in mixed system

To develop one system of white light emission we used a combination of terbium, europium, and gadolinium ions in the same methodology applied to the development of gels. A mixed material was prepared: $Tb_{25\%}Eu_{25\%}Gd_{50\%}$–IL.

The emission spectrum was collected at room temperature with excitation at (1) 350 nm, (2) 355 nm (3) 360 nm (4) 365 nm (5) 370 nm, (6) 375 nm (7) 380 nm (8) 385 nm, (9) and 390 nm (10) 395 nm (Fig. 7A). The obtained emission spectra could be translated into color coordinates on a CIE chromaticity diagram, which is shown in Fig. 7B. The CIE chromaticity diagram shows that the mixed gel exhibited a different color emission irradiating the material with ultraviolet tunable light. Point 4 of the diagram (0356, 0326) suggests that the material is a match in the white light training (0:33, 033). The excitation spectrum of $Tb_{25\%}Eu_{25\%}Gd_{50\%}$–IL, monitoring at 542 nm, shows similar behavior to that shown in Fig. 5, which shows the presence of a broadband and the emission lines. However, when the material is monitored at 616 nm, it reveals a similar pattern found in the spectrum of Fig. 3 with additional lines of terbium ion (Fig. S31). These new signs suggest the energy transfer between from $Tb^{3+}$ to $Eu^{3+}$. As previously reported in the literature, when the $Eu^{3+}$ ion is used as an energy receptor from $Tb^{3+}$, it is common to observe that the luminescence from $Eu^{3+}$ is strongly sensitized to the detriment of $Tb^{3+}$ emission[21].

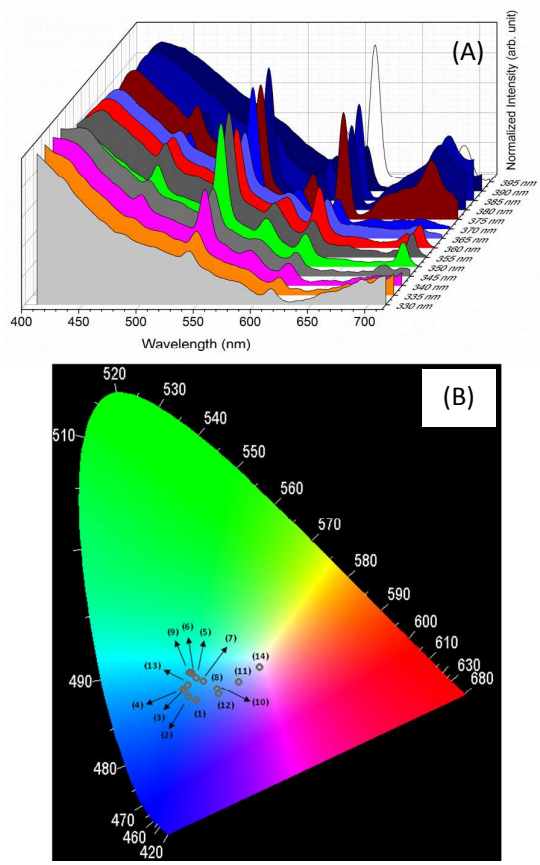


**Fig. 7** CIE diagram points for excitation wavelength in (1) 330 nm, (2) 335 nm (3) 340 nm, (4) 345 nm, (5) 350 nm, (6) 355 nm, (7) 360 nm, (8) 365 nm, (9) 370 nm, (10) 375 nm, (11) 380 nm, (12) 385 nm, (10) 390 nm, (10) 395 nm obtained for $Tb_{25\%}Eu_{25\%}Gd_{50\%}$–IL material.

We note that mixed systems presents similar coordination mode (as evidenced by FTIR shown Fig. S32), and thermal stability (TGA Fig. S33), to above isolated systems (Eu-IL, Tb-IL, Gd-IL).

The great interest in developing ionogels for use in luminescence solar concentrators (LSCs)[15],[16] is justified since these materials can offer a variety of attractive characteristics such as high transparency, outstanding ionic conductivity performance, and the ability to be easily modulated into coatings and monoliths[43]. Furthermore, they provide necessary thermal stability in the operating range of the photovoltaic device. Therefore, the materials developed are potential luminescence solar concentrators once all characteristics presented are mentioned.

## Conclusions

In this paper, we present an efficient methodology to obtain the ionic liquid: 3-methyl-1H-imidazol-3-ium-1-yl) propane-sulfonate with high purity and a yield of 89%, beyond making new supramolecular ionogels based on lanthanide ions ($Eu^{3+}$, $Tb^{3+}$, and $Gd^{3+}$) through heating associate to evaporation, and gentle methodology. We highlight the gentle method with the reaction occurring at room temperature lasting a few minutes with use no solvent. $^{1}$HNMR and FTIR experiments demonstrated self assembly of these gels are accompanied by formation intermolecular hydrogen bonds. The synthesized systems have excellent photophysical properties, such as life time a high, narrow line width and high degree of color purity.

Here, we present an original study for photoluminescence, before the temperature variation, which demonstrates the great photophysics properties to ionogels Eu-IL and Tb-IL. From the theoretical approach we determined the complex geometry of Eu-IL, and the elucidation of energy transfer to photoluminescence mechanisms.

The luminescent color of ionogels can be adjusted by changing the molar ratio of the photoactive units ($Tb^{3+}$/$Eu^{3+}$/$Gd^{3+}$). Subsequently, the white luminescence integration can be presented. Features such as high termal stability (supported by TGA) and reversibility term (evidenced by photoluminescence), confirm that developed materials are potential applications in several areas, such as sensitizers of concentration solar cells (LSCs).

## Acknowledgements

This work was financially supported by FACEPE, CAPES, CNPq (INCT-Inami). We gratefully acknowledge the Department of Fundamental Chemistry for analysis and Danilo Coêlho for collaborations with synthetic methodology. Also, we thank the Pople Computational Chemistry Laboratory for the development and free availability of LUMPAC. We also appreciate the availability of the software Spectra Lux 1.0 by Point Quantum Nanodevices - UFPE research group.

## References

1.Binnemans, K., *Lanthanides and Actinides in Ionic Liquids.* Chem. Rev., 2007. 107: p. 2592−2614.

2.Zhen Ma, J.Y., and Sheng Dai, *Preparation of Inorganic Materials Using Ionic Liquids.* Adv. Mater., 2010. 22: p. 261–285.

3.Dominic Freudenmann, S.W., Michael Wolff, and Claus Feldmann, *Ionic Liquids: New Perspectives for Inorganic Synthesis?* Angew. Chem. Int. Ed., 2011. 50: p. 11050 – 11060.

4.Jin Hong Lee, A.S.L., Jong-Chan Lee, Soon Man Hong, Seung Sang Hwangac and Chong Min Koo, *Hybrid ionogel electrolytes for high temperature lithium batteries.* Journal of Materials Chemistry A, 2015. 3: p. 2226–2233.

5.Huanrong Li, H.S., Yige Wang, Dashan Qin, Binyuan Liu, Wenjun Zhang and Weidong Yan, *Soft material with intense photoluminescence obtained by dissolving $Eu_2O_3$ and organic ligand into a task-specific ionic liquid.* Chem. Commun., 2008: p. 5209–5211.

6.Ling Xu, E.-Y.C., and Young-Uk Kwon, *Combination Effects of Cation and Anion of Ionic Liquids on the Cadmium Metal Organic Frameworks in Ionothermal Systems.* Inorg. Chem., 2008. 47: p. 1907-1909.

7.Maria Bidikoudi, L.F.Z.a.P.F., *Low viscosity highly conductive ionic liquid blends for redox active electrolytes in eficient dye-sensitized solar cells.* J. Mater. Chem. A,, 2014. 2: p. 15326–15336.

8.Bunzli, S.V.E.a.J.-C.G., *Lanthanide luminescence for functional materials and bio-sciences.* Chemical Society Reviews, 2010. 39: p. 189–227.

9.Kyra Lunstroot, K.D., Peter Nockemann, Christiane Gorller-Walrand, Koen Binnemans,Séverine Bellayer, Jean Le Bideau, and André Vioux, *Luminescent Ionogels Based on Europium-Doped Ionic Liquids Confined within Silica-Derived Networks.* Chem. Mater., , 2006. 18: p. 5711-5715.

10.Fan Zhou, T.W., Zhiqiang Li and Yige Wang, *Transparent and luminescent ionogels composed of Eu3+-coordinated ionic liquids and poly(methyl methacrylate).* Luminescence, 2015.

11.Monika Czugala, R.G., Thomas Phelan, Jens Ducree, Dermot Diamond and Fernando Benito-Lopez and *Novel optical sensing system based on wireless paired emitter detector device for lab on a disc water quality analysis* 15th International Conference on Miniaturized Systems for Chemistry and Life Sciences, 2011: p. 1418-1420.

12.Yu Wang, S.K., Yu Zhang, Hengchong Shi, Stephen V. Kershaw, and Andrey L. Rogach, *Thickness-Dependent Full-Color Emission Tunability in a Flexible Carbon Dot Ionogel.* J. Phys. Chem. Lett., 2014. 5: p. 1412−1420.

13.Daeil Kim, G.L., Doyeon Kim, and Jeong Sook Ha, *Air-Stable, High-Performance, Flexible Microsupercapacitor*

*with Patterned Ionogel Electrolyte.* ACS Appl. Mater. Interfaces, 2015: p. A-H.

14.Julia R. Diniz, J.R.C., Daniel de A. Moreira, Rafaela S. Fontenele, Aline L. de Oliveira, Patrícia V. Abdelnur, Jose D. L. Dutra, Ricardo O. Freire, Marcelo O. Rodrigues, and Brenno A. D. Neto, *Water-Soluble $Tb^{3+}$ and $Eu^{3+}$ Complexes with Ionophilic (Ionically Tagged) Ligands as Fluorescence Imaging Probes.* Inorganic Chemistry, 2013: p. A-G.

15.Huifang Wang, Y.W., Li Zhang and Huanrong Li, *Transparent and luminescent ionogels based on lanthanide-containing ionic liquids and poly(methylmethacrylate) prepared through an environmentally friendly method.* RSC Advances, 2013. 3: p. 8535–8540.

16.Jing Zhang, W.Z., Jiangna Guo, Chao Yuan, Feng Yan, *Ultrahigh Ionic Liquid Content Supramolecular Ionogels for Quasi-Solid-State Dye Sensitized Solar Cells.* Electrochimica Acta, 2015. 165: p. 98–104.

17.Renata Reisfeld, D.S., Christian Jorgensen, *Photostable solar concentrators based on fluorescent glass films* Solar Energy Materials and Solar Cells 1994. 33: p. 417-427.

18.Meredith G. Hyldahl, S.T.B., Bruce P. Wittmershaus, *Photo-stability and performance of CdSe/ZnS quantum dots in luminescent solar concentrators.* Solar Energy 2009. 83: p. 566–573.

19.Vania. T. Freitas, L.F., Ana M. Cojocariu, Xavier Cattoen, John R. Bartlett, Rozenn Le Parc, Jean-Louis Bantignies, Michel Wong Chi Man, Paulo S. Andre, Rute A. S. Ferreira, and Luís D. Carlos, *$Eu^{3+}$ Based Bridged Silsesquioxanes for Transparent Luminescent Solar Concentrators.* Appl. Mater. Interfaces, 2015: p. A-I.

20.Chang, H.K.a.J.Y., *White light emission from a mixed organogel of lanthanide(III)-containing organogelators.* RSC Advances, 2013. 3: p. 1774–1780.

21.Marcelo O. Rodrigues, J.D.L.D., Luiz Antonio O. Nunes, Gilberto F. de Sa, Walter M. de Azevedo, Patrícia Silva, Filipe A. Almeida Paz, Ricardo Oliveira Freire, and Severino A. Junior, *$Tb^{3+}$→$Eu^{3+}$ Energy Transfer in Mixed-Lanthanide-Organic Frameworks.* J. Phys. Chem. C, 2012. 116: p. 19951−19957.

22.Jose Diogo L. Dutra, T.D.B., and Ricardo O. Freire, *LUMPAC Lanthanide Luminescence Software: Efficient and User Friendly.* Journal of Computational Chemistry, 2014. 35: p. 772–775.

23.Manoel A. M. Filho, J.D.L.D., Gerd B. Rocha, Alfredo M. Simas, Ricardo O. Freire, *Semiempirical Quantum Chemistry Model for the Lanthanides: RM1 (Recife Model 1) Parameters for Dysprosium, Holmium and Erbium.* Plos One, 2014. 9(1): p. 1-10.

24.Binnemans, K., *Interpretation of europium(III) spectra.* Coordination Chemistry Reviews, 2015. 295: p. 1–45.

25.Rodrigues, M.O., *Estudos Espectroscópicos de Materiais Metal-Orgânicos baseados em Íons Lantanídeos* in *Doutorado em Química* 2010 Universidade Federal de Pernambuco: Recife. p. 222.

26.George K. H. Shimizu, R.V.a.J.M.T., *Phosphonate and sulfonate metal organic frameworks.* Chem. Soc. Rev., 2009. 38: p. 1430–1449.

27.Köckerling, T.P.a.M., *Imidazolium-Based Zwitterionic Butane-1-sulfonates: Synthesis and Properties of 4-(1-(2-Cyanoethyl)imidazolium)butane-1-sulfonate and Crystal Structures of 4-(1-Alkylimidazolium)butane-1-sulfonates (Alkyl = Methyl, Ethyl, Propyl).* Z. Anorg. Allg. Chem., 2011. 637: p. 870–874.

28.Hua Li, J.L., Jiang Zhu, and Hongkai Wang, *Preparation of Novel Ionic Liquids and Their Applications in Brominating Reaction.* Journal of the Korean Chemical Society, 2011. 55: p. 685-690.

29.Jong Hwa Jung, S.S., and Toshimi Shimizu, *Spectral Characterization of Self-Assemblies of Aldopyranoside Amphiphilic Gelators: What is the Essential Structural Difference between Simple Amphiphiles and Bolaamphiphiles?* Chem. Eur. J., 2002. 8: p. 2684-2690.

30.W. Matthew Reichert, P.C.T.a.H.C.D.L., *3-(1-Methyl-3-imidazolio)propane-sulfonate: a precursor to a Brønsted acid ionic liquid.* Acta Crystallographica Section E, 2010. E66: p. o591.

31.Stern, K.H., *High Temperature Properties and Decomposition of Inorganic Salts Part 3. Nitrates and Nitrites.* J. Chem. Phys., 1972. 1: p. 746-772.

32.Abiodun O. Eseola, W.L., Wen-Hua Sun, Min Zhang, Liwei Xiao, Joseph A.O. Woods, *Luminescent properties of some imidazole and oxazole based heterocycles: Synthesis, structure and substituent effects.* Dyes and Pigments 2011. 88: p. 262-273.

33.G. Blasse, B.C.G., *Luminescent Materials.* Springer-Verlag, 1994. 34.Alex S. Borges, J.D.L.D., Ricardo O. Freire, Renaldo T. Moura, Jr., Jeferson G. Da Silva, Oscar L. Malta, Maria Helena Araujo, and Hermi F. Brito, *Synthesis and Characterization of the Europium(III) Pentakis(picrate) Complexes with Imidazolium Countercations: Structural and Photoluminescence Study.* Inorganic Chemistry 2012. 51: p. 12867−12878.

35.Martinus H. V. Werts, R.T.F.J.a.J.W.V., *The emission spectrum and the radiative lifetime of $Eu^{3+}$ in luminescent lanthanide complexes.* Phys. Chem. Chem. Phys., 2002. 4: p. 1542–1548.

36.King, R.B., *The Shapes of Coordination Polyhedra.* Journal of Chemical Education, 1996. 73: p. 993-997.

37.M.E. de Mesquita, F.R.G.e.S., R.Q. Albuquerque, R.O. Freire, E.C. da Conceição, J.E.C. da Silva, N.B.C. Júnior, and G.F.deSá *Eu(III) and Gd(III) complexes with pirazyne-2-carboxylic acid: luminescence and modelling of the structure and energy transfer process.* Journal of Alloys and Compounds 2004. 366: p. 124–131.

38.Janina Legendziewicz , P.G., Ewa Gałdecka , Zdzislaw Gałdecki, *Novel polynuclear compound of europium with N-phosphonomethylglycine: spectroscopy and*

*structure.* Journal of Alloys and Compounds 1998: p. 356–360.

39.Jun-Ling Song, C.L., and Jiang-Gao Mao, *Syntheses, Crystal Structures, and Luminescent Properties of Novel Layered Lanthanide Sulfonate−Phosphonates.* Inorg. Chem. , 2004. 43: p. 5630−5634.

40.Julio G. Santos, J.D.L.D., Severino A. Junior, Ricardo O. Freire, and Nivan B. da Costa Junior, *Theoretical Spectroscopic Study of Europium Tris(bipyridine) Cryptates.* J. Phys. Chem. A, 2012. 116: p. 4318−4322.

41.Wagner E. Silva, M.F.B., Ricardo O. Freire, Gilberto F. de Sa, and Severino Alves Jr. , *New Homotrinuclear Lanthanide Complexes: Synthesis, Characterization and Spectroscopic Study.* J. Phys. Chem. A 2010. 114: p. 10066–10075.

42.Lippy F. Marques, C.C.C., Sidney J.L. Ribeiro, Molíria V. dos Santos, José Diogo L. Dutra, Ricardo O. Freire, Flávia C. Machado *Synthesis, structural characterization, luminescent properties and theoretical study of three novel lanthanide metal-organic frameworks of Ho(III), Gd(III) and Eu(III) with 2,5-thiophenedicarboxylate anion.* Journal of Solid State Chemistry 2015. 227: p. 68–78.

43.Zengpeng Fan, Y.W., Zhixin Xue, Li Zhang, Yuhuan Chen, Shuming Zhang, *Preparation, characterization and luminescence of transparent thin film of ionogels.* J Sol-Gel Sci Technol 2014. 72: p. 328–333.

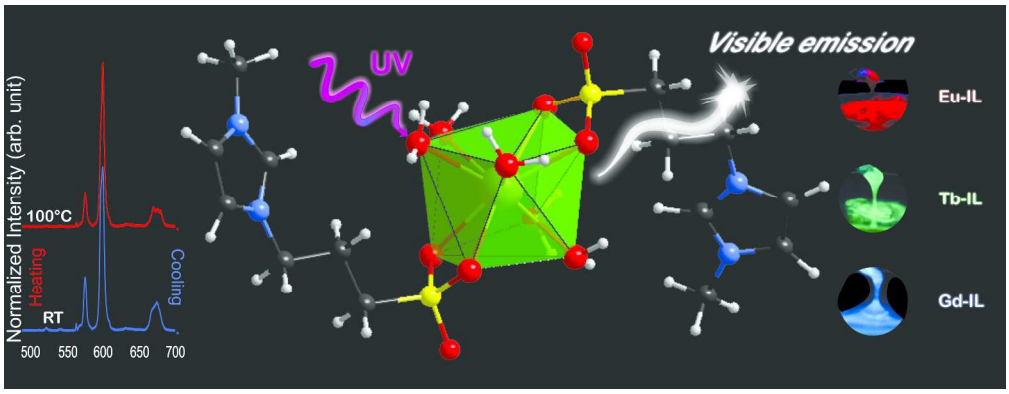


269x103mm (300 x 300 DPI)